ELSEVIER

Materials Science and Engineering B69–70 (2000) 227–231

MATERIALS SCIENCE & ENGINEERING B

www.elsevier.com/locate/mseb

Application of Nd:YLF laser to amorphous silicon crystallization process

P. delli Veneri *, M.L. Addonizio, A. Imparato, C. Minarini, C. Privato, E. Terzini

Centro Ricerche ENEA, Loc. Granatello, I-80055 Portici, Italy

Abstract

Polysilicon thin films have been obtained by Laser Induced Crystallization utilizing a Q-switched diode pumped, frequency-doubled Nd:YLF laser at 523-nm wavelength. Intrinsic and n-doped amorphous materials, of different thickness, have been deposited on Corning 1737 by LPCVD technique. The irradiation conditions have been varied in order to study their influence on crystallized material properties. Electrical and optical properties of as-deposited and crystallized films have been determined. Structural characterization has been performed to evaluate average grain size and distribution. Larger grain size has been observed in intrinsic materials compared to n-doped materials and the largest grain size (≈ 1 μm) has been obtained on materials having thickness of 50 nm. Critical role of doping in the crystallization process has been pointed out. © 2000 Elsevier Science S.A. All rights reserved.

Keywords: Crystallization; Polycrystalline; Laser irradiation; Grain size

1. Introduction

Polycrystalline silicon thin film transistors (polySi-TFTs) realized by crystallization of amorphous silicon have been recognized as the basis of the AMLCD technology in the next future. Polycrystalline silicon TFTs field effect mobility, differently from a-Si based ones, can reach a value larger than 100 $cm^2\ V\ s^{-1}$[1]. This is the threshold to get over to build both switching elements and driving circuitry of an AMLCD by the same material on a monolithic substrate, obtaining a notable improvement of the industrial process efficiency. Moreover, the same material can be a suitable photovoltaic material for the realization of degradation free low cost solar cells [2–4]. Although amorphous silicon can be successfully crystallized on inexpensive glass substrates, such as Corning 1737, by standard and well-established thermal solid phase crystallization (SPC), the time required for a glass compatible temperature is very long. As a consequence, high relevance has the development of glass compatible crystallization technologies, more industrial attractive in terms of productivity and economy, such as laser induced crystallization (LIC). The laser light absorption phenomenon allows very high temperature localized in the film, leading to crystallization, while the substrate temperature keeps at a glass compatible value.

Polycrystalline silicon thin film for TFTs usually is performed by using excimer laser [5] but, due to the short wavelength and the related high absorption coefficient of silicon, the thickness that can be crystallized with this laser is less than 100 nm. In order to crystallize thicker layers of amorphous silicon longer wavelength lasers need to be used [6]. The possibility to crystallize larger thickness can be interesting if one wants to use this layer as a crystallographic template in order to epitaxially grow an absorber film with a thickness of a few microns. Theoretical studies [7] show that thin film polycrystalline Si solar cells have the potential to attain an attractive efficiency only if film thickness is larger than 2 μm.

In this work we present the characteristics of samples crystallized by Nd:YLF laser having a wavelength of 523 nm. Different irradiation conditions have been utilized in order to optimize the structural film properties. Various amorphous silicon starting materials have been investigated leading to different grain size.

* Corresponding author. Tel.: +39-081-7723259; fax: +39-081-7723344.

E-mail address: delliveneri@epoca1.portici.enea.it (P. delli Veneri)

0921-5107/00/$ - see front matter
PII: S0921-5107(99)00300-1

2. Experimental

A horizontal quartz tube has been utilized for the deposition of amorphous silicon on Corning 1737 by LPCVD technique. The process utilizes pure SiH_4 or PH_3/SiH_4 gas mixture at a pressure of 350 mTorr and a furnace temperature of 570°C. Gas phase doping ratio (PH_3/SiH_4) has been varied between 0.1 and 1%. The growth rate is in the range of 2–3 nm min^{-1} and the film thickness ranges from 50 to 200 nm.

Table 1
Optical and electrical data of a-Si films utilized in this study

Samples	E_g (eV)	σ (S cm^{-1})
Intrinsic	1.50	8×10^{-7}
n-doped (PH_3/SiH_4 = 0.1%)	1.49	6.5×10^{-2}
n-doped (PH_3/SiH_4 = 1%)	1.47	1.9×10^{-1}

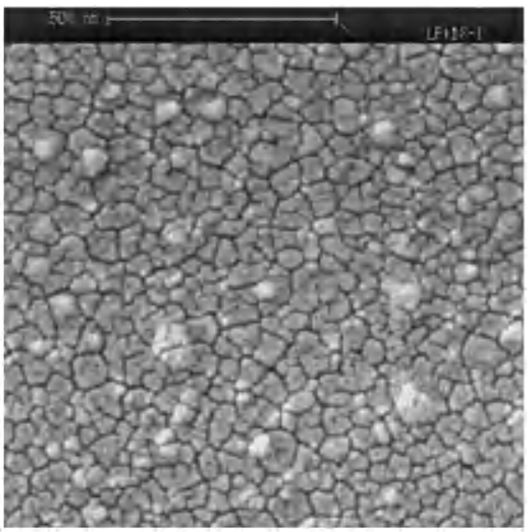

Fig. 1. SEM micrograph of an intrinsic film having thickness of 50 nm crystallized at 490 mJ cm^{-2} with an overlapping of 80%.

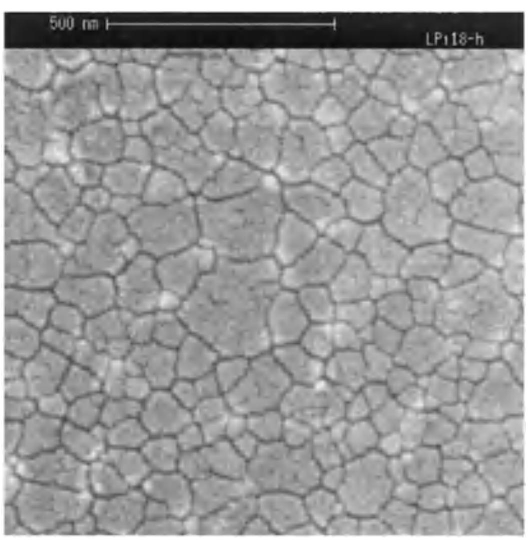

Fig. 2. SEM micrograph of an intrinsic film having thickness of 50 nm crystallized at 490 mJ cm^{-2} with an overlapping of 90%.

A Q-switched diode pumped, frequency-doubled Nd:YLF laser at 523-nm wavelength, having a maximum power of about 0.2 W and a pulse width of 30 ns at a repetition rate of 2000 Hz, has been used for crystallization process. The laser beam has been focused on the sample by a cylindrical lens resulting in beam dimensions of 16 mm $\times$ 12 μm. The energy density per pulse has been varied from 490 to 590 mJ cm^{-2}. The samples, positioned on a translation stage, have been irradiated in air, at room temperature. The stage scanning velocity and the laser repetition rate have been adjusted in order to obtain an overlapping (percentage of superposition of two successive shots) of irradiated area from 80 to 90%.

Amorphous and crystallized samples have been characterized by optical transmission utilizing a Perkin Elmer λ-9 UV/VIS/NIR spectrophotometer in the 250–2500 nm wavelength range for optical absorption coefficient and energy gap (E_g) determination. Presence of ordered phase has been detected by means of UV reflectance measurements. Conductivity values have been measured by four probe technique or metal coplanar contacts.

Crystallite size has been determined by XRD measurements that have been carried out with an MPD-X'PERT (Philips) diffractometer using a Cu K_α radiation source.

Film morphology and average grain size have been determined by Scanning Electron Micrograph (SEM) analysis. The grains boundaries have been visualized by anisotropic etching using Secco etching solution. Computer image analysis has been utilized to determine the grains area, the equivalent circle diameter and the grain size distribution.

3. Results and discussion

The optical and electrical properties of amorphous starting films are summarized in Table 1. Energy gap (E_g) typical of dehydrogenated a-Si materials has been achieved together with high conductivity values for the doped films.

3.1. Crystallized intrinsic films

Figs. 1–3 show SEM micrograph of three crystallized intrinsic films having a thickness of 50 nm. Figs. 1 and 2 report the morphology of samples irradiated at the same energy density (490 mJ cm^{-2}) with overlapping values of 80 and 90% respectively. The sample of Fig. 3 has been crystallized at 590 mJ cm^{-2} with the same overlapping (90%) utilized for the sample of Fig. 2. The

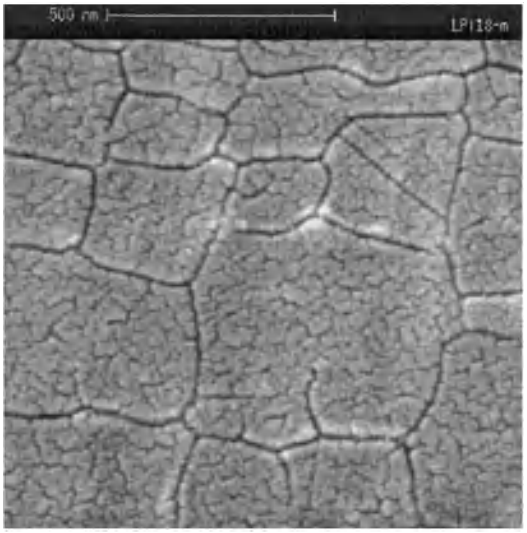

Fig. 3. SEM micrograph of an intrinsic film having thickness of 50 nm crystallized at 590 mJ cm^{-2} with an overlapping of 90%.

comparison points out that, at 490 mJ cm^{-2} per pulse, an increase of overlapping causes an increase of grain dimensions (Fig. 1 vs. Fig. 2). The largest grains are about 150 and 210 nm with 80 and 90% of overlapping respectively. With an overlapping value of 90%, larger grain size is obtained at the highest energy value (Fig. 2 vs. Fig. 3).

In this case a large grain distribution can be distinguished with grains reaching size up to 900 nm (see Table 2). This behavior could agree with a crystallization process in which the laser energy density is able to melt the amorphous material that crystallizes following an explosive crystallization. Successive pulses melt the fine-grained material leaving some crystalline cluster seeds, poorly dispersed in the liquid. In this condition, around those seeds, it is possible to have the growth of grains that are many times greater than the film thickness with a reduced homogeneous nucleation [8]. This mechanism may explain the observed crystallization that could be seen as a mixing of Super Lateral Growth (SLG) and explosive phenomena.

The effect of amorphous film thickness on the crystallization process has been investigated at the laser condition optimized on 50-nm thick film (energy density of 590 mJ cm^{-2} and overlapping 90%).

Table 2 summarizes the results of this investigation together with the main data of crystallization experiments. The data show that the increase of thickness causes a reduction of the average grain size but also a narrowing of grain size distribution. The reduction of grain size could be in agreement with a partial material melting during successive irradiation pulses.

The film structure has been determined by XRD measurements in $\Theta - 2\Theta$ and grazing angle configurations; the grazing angle technique has been utilized in order to enhance the film signal with respect to the Corning substrate and accurately quantify the crystalline phase. Fig. 5 (bottom spectrum) shows XRD spectra of the 200-nm thick film listed in Table 2. The measurement confirms the total crystallization of the material with a random orientation. The average crystallite size, calculated by Debye–Scherrer formula, is about 50 nm.

3.2. Crystallized phosphorus doped films

Different results have been achieved for n-doped materials crystallized in the same conditions of intrinsic films. In Fig. 4 a SEM micrograph of a doped film crystallized at 590 mJ cm^{-2} and at 90% of overlapping is shown. The grain size is small (40–50 nm); this result does not change by varying the laser energy densities and there is no influence of the gas phase doping level.

Film structural data from XDR measurements are always reported in Fig. 5. No change in the spectra as a function of the gas phase doping concentration (0.1% and 1%) has been observed. Also in this case the films show random orientation and an average crystallite size of about 50 nm.

The smaller grain size observed in the P doped films in comparison to the intrinsic ones could be ascribed to the laser crystallization mechanism or to the role of the doping atoms in the nucleation phenomenon.

Other authors have studied the effect of doping in crystallization processes. In particular, controversial effects of P atoms concentration on the grain size of solid

Table 2
Data of crystallized intrinsic films under different conditions of irradiation

Thickness (nm)	Energy density (mJ cm^{-2})	Overlapping (%)	Maximum grain size (nm)	Average grain size (nm)	S.D. (nm)
50	490	80	149	63	25
50	490	86	165	73	28
50	490	90	208	77	29
50	540	90	374	189	67
50	590	90	911	255	132
100	590	90	323	133	59
200	590	90	167	82	32

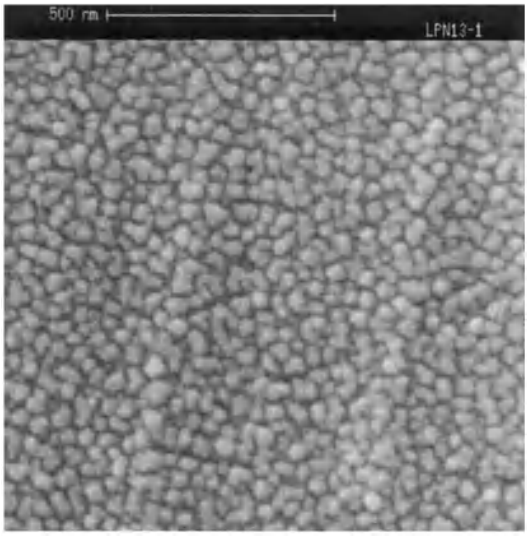

Fig. 4. SEM micrograph of a doped film having thickness of 50nm crystallized at 590 mJ cm^{-2} with an overlapping of 90%.

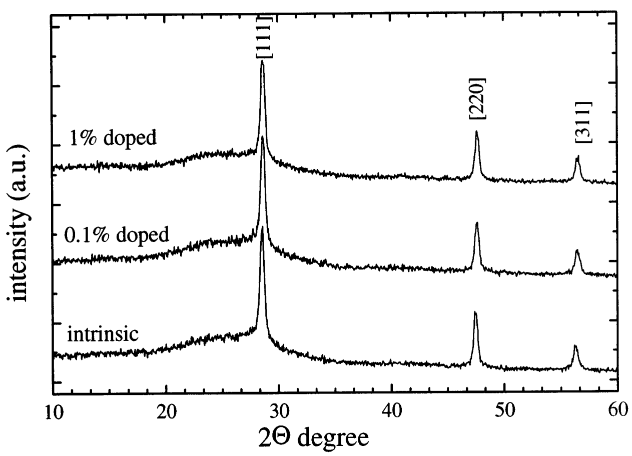

Fig. 5. XRD spectra of intrinsic, 0.1 and 1% doped crystallized films.

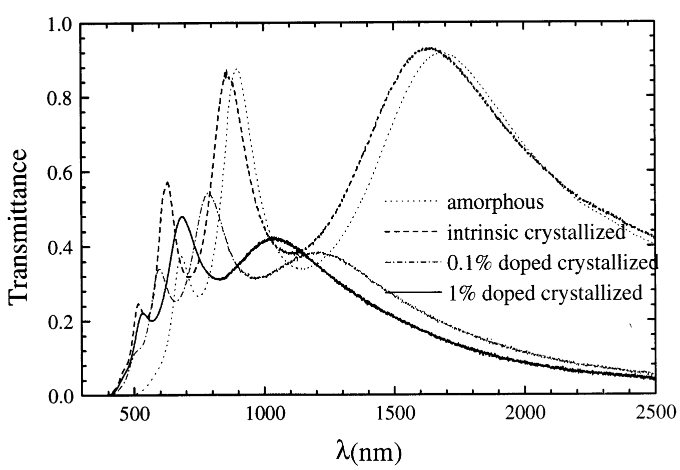

Fig. 6. Transmittance spectra of different crystallized films and of a LPCVD amorphous material.

phase crystallized (SPC) material have been reported [9,10]. Nevertheless, we have utilized the SPC as comparative crystallization technique in order to make out if the detrimental effect on the grain size has to be ascribed to the doping concentration or to the selected crystallization process. To this aim, we have treated the intrinsic and P doped amorphous films with an isothermal annealing in a furnace, under vacuum condition, at 600°C for 15 h.

The result of our SPC process does not differ from what we achieved by laser crystallization: intrinsic films have grain size about 10 times larger than doped materials (400 and 40 nm respectively). Hence, in our doped material, the small grain size of the crystallized doped film seems not to depend on the process utilized for crystallization.

Our doped films are characterized by a high phosphorous content that can be inferred from the conductivity values of LPCVD n-type materials and from the behavior of optical transmittance. Fig. 6 reports the transmittance spectra of amorphous and crystallized samples having thickness of 200 nm. Beside the differences of transmittance between amorphous and crystallized silicon in the high energy region due to the different E_g, it can be noted, in the doped samples, a reduced transmittance starting in the visible region and extending more strongly at longer wavelengths. This is the fingerprint of absorption by free carriers whose density is in the 10^{21} cm^{-3} range, on the basis of optical absorption value in the near IR region [11]. Therefore we can infer that laser crystallization of doped material is strongly governed by the large density of phosphorous atoms. When the melted material contains large amount of impurity atoms in excess with respect to the solid solubility limit [12], the rapid cooling of the melt causes the formation of P atoms precipitates that give rise to a large density of nucleation sites. The increase of nucleation sites in doped films with respect to intrinsic films determines the observed decrease of grain size. Furthermore the activation of large number of P atoms upon laser crystallization is pointed out by the high conductivity of n-type crystallized samples showing values of 1.5×10^3 and 2×10^3 S cm^{-1} for 0.1 and 1% gas doping respectively.

On the other hand, the small grain size we achieved by SPC of doped films, also observed by others in correspondence of high doping concentration [10], could be explained by the formation of an ordered microstructure in the starting amorphous material. This is confirmed from UV reflectance measurements carried out on our amorphous films. Fig. 7 illustrates reflectance spectra of an intrinsic and doped amorphous films and, for comparison, a spectrum of a polycrystalline film. The presence of an ordered phase is revealed by the reflectance peak at 275 nm due to direct optical transition in the k-space [13], which shows an

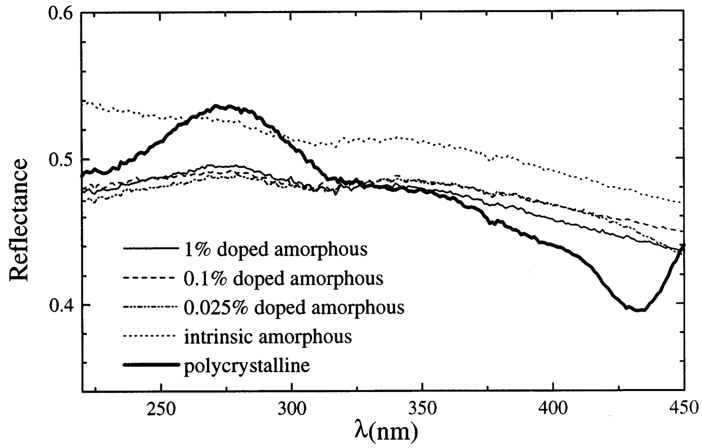

Fig. 7. UV reflectance spectra of an intrinsic and n doped a-Si films. For comparison, a spectrum of a polycrystalline sample is reported.

increase along with the doping concentration. XRD measurements performed on the same samples are not able to identify an ordered structure. Nevertheless the evidence of the optical measurements lets to infer that the resolved nanostructure could form a homogeneous distribution of nucleation sites with the consequence of the small grain size in the fully crystallized samples.

4. Conclusions

Crystallization of LPCVD amorphous silicon has been achieved by utilizing a Nd:YLF pulsed laser at a wavelength of 523 nm. The effect of laser energy density and beam overlapping on both intrinsic and doped films of different thickness have been investigated. An intermediate regime of SLG and explosive crystallization, giving grain size of about 1 μm, has been identified on 50 nm thick films. Doped and intrinsic laser crystallized films show the same crystallite size when analyzed by XRD. The larger grain size of crystallized i-layers with respect to P doped films has been ascribed to the very high doping concentration of the starting material. Analogous effect of phosphorous concentration on SPC crystallized films has been also pointed out and ascribed to a nanocrystalline structure of our starting LPCVD films. The investigation indicates that a suitable increase of grain size for doped materials can only be achieved by a careful control of the doping atoms in the solid phase. Further investigations about optical and electrical properties of the crystallized films are needed in order to evaluate the actual device quality of the produced material. Nevertheless in this work we have demonstrated the possibility to utilize Nd:YLF laser to produce a polycrystalline material with good structural properties.

Acknowledgements

The authors thank A. Rubino for helpful discussion. This work has been supported by European Community with ERDF founds, under the Italian Scientific and Technological Research and University Ministry coordination.

References

[1] S.D. Brotherton, Semicond. Sci. Technol. 10 (1995) 721.
[2] R. Bergmann, G. Oswald, M. Albrecht, J.H. Werner, Solid State Phenom. 51/52 (1995) 515.
[3] T. Baba, M. Shima, T. Matsuyama, S. Tsuge, K. Wasisaka, S. Tsuda, Proceedings of the 13th EC PVSEC, 1995, p. 1708.
[4] A.V. Shah, J. Meier, P. Torres, U. Kroll, D. Fischer, N. Beck, N. Wyrsch, H. Keppner, Proceedings of the 26th IEEE Conference, 1997, p. 569.
[5] H.J. Kim, J.S. Im, Appl. Phys. Lett. 68 (1996) 1513.
[6] G. Andra, J. Bergmann, F. Falk, E. Ose, H. Stafast, Proceedings of the 185 International WE–Heraeus Workshop, 1998, p. 629.
[7] M. Imaizumi, T. Ito, M. Yamaguchi, K. Kaneko, J. Appl. Phys. (1997) 7635.
[8] J.S. Im, H.J. Kim, Appl. Phys. Lett. 64 (1994) 2303.
[9] R.B. Bergmann, J. Krinke, J Crystal Growth (1997) 191.
[10] T. Matsuyama, K. Wakisava, M. Kameda, M. Tanaka, T. Matsuoka, S. Tsuda, S. Nakano, Y. Kishi, Y. Kuwano, Jpn. J. Appl. Phys. 29 (1990) 2327.
[11] R.A. Soref, B.R. Bennett, IEEE J. Quantum Electron. 23 (1987) 123.
[12] N. Inoue, J. Osaka, K. Wada, J. Electrochem. Soc. 129 (1982) 2780.
[13] F. Bassani, G. Pastori Parravicini, Electronic States and Optical Transition in Solids, Pergamon, Oxford, 1975.